Cebranopadol: A Novel Potent Analgesic Nociceptin/Orphanin FQ Peptide and Opioid Receptor Agonist[S]

Klaus Linz, Thomas Christoph, Thomas M. Tzschentke, Thomas Koch, Klaus Schiene, Michael Gautrois, Wolfgang Schröder, Babette Y. Kögel, Horst Beier, Werner Englberger, Stefan Schunk, Jean De Vry, Ulrich Jahnel, and Stefanie Frosch

Departments of Preclinical Drug Safety (K.L.), Global Preclinical Drug Development (S.F.), Global Preclinical Research and Development (U.J.), Pain Pharmacology (T.C., T.M.T., K.S., B.Y.K., J.D.V.), Molecular Pharmacology (T.K., W.E.), Translational Science (W.S.), Pharmacokinetics (M.G., H.B.), and Medicinal Chemistry (S.S.), Grünenthal GmbH, Aachen, Germany

Received February 23, 2014; accepted April 7, 2014

ABSTRACT

Cebranopadol (*trans*-6′-fluoro-4′,9′-dihydro-*N,N*-dimethyl-4-phenyl-spiro[cyclohexane-1,1′(3′H)-pyrano[3,4-b]indol]-4-amine) is a novel analgesic nociceptin/orphanin FQ peptide (NOP) and opioid receptor agonist [K_i (nM)/EC_{50} (nM)/relative efficacy (%): human NOP receptor 0.9/13.0/89; human mu-opioid peptide (MOP) receptor 0.7/1.2/104; human kappa-opioid peptide receptor 2.6/17/67; human delta-opioid peptide receptor 18/110/105]. Cebranopadol exhibits highly potent and efficacious antinociceptive and antihypersensitive effects in several rat models of acute and chronic pain (tail-flick, rheumatoid arthritis, bone cancer, spinal nerve ligation, diabetic neuropathy) with ED_{50} values of 0.5–5.6 μg/kg after intravenous and 25.1 μg/kg after oral administration. In comparison with selective MOP receptor agonists, cebranopadol was more potent in models of chronic neuropathic than acute nociceptive pain. Cebranopadol's duration of action is long (up to 7 hours after intravenous 12 μg/kg; >9 hours after oral 55 μg/kg in the rat tail-flick test). The antihypersensitive activity of cebranopadol in the spinal nerve ligation model was partially reversed by pretreatment with the selective NOP receptor antagonist J-113397[1-[(3R,4R)-1-cyclooctylmethyl-3-hydroxymethyl-4-piperidyl]-3-ethyl-1,3-dihydro-2H-benzimidazol-2-one] or the opioid receptor antagonist naloxone, indicating that both NOP and opioid receptor agonism are involved in this activity. Development of analgesic tolerance in the chronic constriction injury model was clearly delayed compared with that from an equianalgesic dose of morphine (complete tolerance on day 26 versus day 11, respectively). Unlike morphine, cebranopadol did not disrupt motor coordination and respiration at doses within and exceeding the analgesic dose range. Cebranopadol, by its combination of agonism at NOP and opioid receptors, affords highly potent and efficacious analgesia in various pain models with a favorable side effect profile.

Introduction

Almost 20 years ago, a new member of the opioid receptor family and its endogenous agonist were described (Meunier et al., 1995; Reinscheid et al., 1995). Because of its partial homology to the opioid receptors [mu-opioid peptide (MOP) receptor, delta-opioid peptide (DOP) receptor, kappa-opioid peptide (KOP) receptor] and its insensitivity to the prototypical opioid agonist and antagonist ligands morphine and naloxone, this receptor was initially termed opioid receptor-like receptor,

ORL1. Subsequently, it was renamed the nociceptin/orphanin FQ peptide (NOP) receptor after its endogenous ligand nociceptin, and it is now considered to be a non-opioid member of the opioid receptor family (Cox et al., 2009). At a cellular level, the actions of the NOP receptor are broadly similar to those of the opioid receptors (Chiou et al., 2007; Lambert, 2008). Although NOP receptors are clearly expressed at all levels of the pain pathways, it is thought that NOP and MOP receptors are not colocalized in the same neurons and may, thus, have independent actions in at least partly distinct neuronal networks (Monteillet-Agius et al., 1998).

The role of the NOP receptor in pain and analgesia has remained unclear for some time owing to inconsistent findings in early reports using nociceptin to activate the receptor. Being a peptide, nociceptin was administered locally into the central

ABBREVIATIONS: [³H]DAMGO, (D-Ala₂,*N*-Me-Phe₄, glycinol₅)-enkephalin; 5-HT, serotonin; ANOVA, analysis of variance; BL, baseline; CCI, chronic constriction injury; CFA, complete Freund's adjuvant; CI, confidence interval; CI-977, enandoline [(5R)-(5α,7α,8β)-*N*-methyl-*N*-[7-(1-pyrrilidinyl)-1-oxaspiro [4,5]dec-8-yl-4-benzofuranacetamide monohydrochloride]; CNS, central nervous system; DMSO, dimethylsulfoxide; DOP, delta opioid peptide; E_{max}, maximum possible effect for the agonist; EVF, electronic von Frey; GTPγS, guanosine-5′-[γ-thio]triphosphate; J-113397, 1-[(3R,4R)-1-cyclooctylmethyl-3-hydroxymethyl-4-piperidyl]-3-ethyl-1,3-dihydro-2H-benzimidazol-2-one; KOP, kappa-opioid peptide; MOP, mu-opioid peptide; MPE, maximum possible effect; NOP, nociceptin/orphanin FQ peptide; Ro64-6198, 8-[(1S,3aS)-2,3,3a,4,5,6-hexahydro-1*H*-phenalen-1-yl]-1-phenyl-1,3,8-triaza-spiro[4.5]decan-4-one; SNC 80, (+)-4-[(αR)-α-((2S,5R)-4-Allyl-2,5-dimethyl-1-piperazinyl)-3-methoxybenzyl]-*N,N*-diethylbenzamide; SNL, spinal nerve ligation; STZ, streptozotocin; U69,593, (+)-(5α,7α,8β)-*N*-Methyl-*N*-[7-(1-pyrrolidinyl)-1-oxaspiro[4.5]dec-8-yl]-benzeneacetamide.

nervous system (CNS) where it produced both pronociceptive and antinociceptive effects when administered supraspinally (Meunier et al., 1995; Calo and Guerrini, 2013). Remarkably, when administered into the spinal cord of rodents and nonhuman primates, nociceptin consistently produced antinociceptive effects (Ko et al., 2009; Sukhtankar and Ko, 2013). Subsequent studies of systemic administration of nonpeptide NOP receptor agonists revealed that such compounds were effective analgesics in animal pain models. Although evidence for antinociceptive and antihyperalgesic effects in rodents is limited and inconsistent (Jenck et al., 2000; Reiss et al., 2008), Ko et al. (2009) demonstrated impressive antinociceptive and antiallodynic potency and efficacy using the NOP receptor agonist Ro64-6198 in Rhesus monkeys. Potency and efficacy were comparable with those of alfentanil but with a complete absence of alfentanil-associated side effects such as itching/scratching and respiratory depression and no evidence of reinforcing effects (Ko et al., 2009; Podlesnik et al., 2011).

Currently, strong MOP receptor agonists are the most effective drugs for the treatment of moderate to severe acute and chronic pain. However, although these drugs provide potent analgesia, they also carry the risk of severe side effects such as respiratory depression, nausea, vomiting, and constipation, and their use may lead to physical dependence and tolerance (Zöllner and Stein, 2007). In addition, opioids are considered to have limited efficacy in treating chronic nociceptive and neuopathic pain owing to a reduction in the already low therapeutic index (Rosenblum et al., 2008; Labianca et al., 2012). For these reasons, there is an unmet medical need for potent and well-tolerated analgesics for the treatment of moderate to severe chronic nociceptive and neuropathic pain.

As NOP and opioid receptor agonists modulate pain and nociception via distinct yet related targets, combining both mechanisms may constitute an interesting and novel approach for the development of innovative analgesics. Notably, a supra-additive interaction between intrathecal morphine and intrathecal nociceptin has been described in rodents (Courteix et al., 2004), as well as an enhancement of the antinociceptive effect of systemic morphine by systemic administration of Ro64-6198 (Reiss et al., 2008). Furthermore, a synergistic effect of concurrent NOP and MOP receptor activation without significant side effects has been demonstrated in nonhuman primates after systemic administration (Cremeans et al., 2012). At the same time, activation of NOP receptors has been proposed to counteract supraspinal opioid activity; in animal studies, NOP receptor agonists do not generate typical opioid-like side effects and may even ameliorate opioid-related side effects when administered concurrently with an opioid agonist (Ko et al., 2009; Rutten et al., 2010; Toll, 2013). Thus, a combination of NOP and opioid receptor activation may be particularly suited to provide potent analgesia with reduced opioid-like side effects.

To explore the potential benefits of NOP and opioid receptor coactivation, novel compounds acting as agonists on both NOP and opioid receptors have been designed (Molinari et al., 2013; Zaveri et al., 2013). This article describes the preclinical pharmacology of cebranopadol (Fig. 1), a potent NOP and opioid receptor agonist derived from a novel chemical series of spiro [cyclohexane-dihydropyrano[3,4-b]indol]-amines (S. Schunk, K. Linz, C. Hinze, S. Frormann, S. Oberbörsch, B. Sundermann, S. Zemolka, W. Englberger, T. Germann, T. Christoph, B.Y. Kögel, W. Schröder, S. Harlfinger, D. Saunders, A. Kless, H. Schick, and
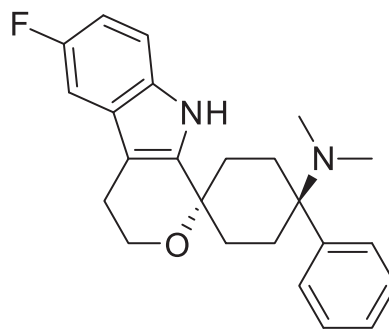

Fig. 1. Chemical structure of *trans*-6′-fluoro-4′,9′-dihydro-*N*,*N*-dimethyl-4-phenyl-spiro[cyclohexane-1,1′(3′*H*)-pyrano[3,4-b]indol]-4-amine (cebranopadol).

H. Sonnenschein, submitted manuscript) that was developed by Grünenthal (Aachen, Germany) and is currently in clinical development for the treatment of severe chronic pain.

Materials and Methods

Animals

In Vitro Studies. Membrane suspensions used for rat brain receptor binding studies were obtained from male Sprague-Dawley specific-pathogen-free rats (average weight 200 g) (Charles River Laboratories, Sulzfeld, Germany).

In Vivo Studies. Behavioral studies in pain models and pharmacokinetic evaluations were conducted in Sprague-Dawley rats (weight range 134−423 g; tail-flick model: Iffa Credo, Brussels, Belgium; bone cancer model: Harlan Laboratories, Indianapolis, IN; all other pain models and pharmacokinetics: Janvier Laboratories, Le Genest Saint Isle, France); male rats were used for most of the experiments, except for the tail-flick and bone cancer models, for which female Sprague-Dawley rats were used. Studies in side effect models were conducted in male Wistar rats (weight range 150−375 g; Dépré, Saint Doulchard, France). Rats were housed under standard conditions (room temperature 20−24°C, 12 hour light/dark cycle, relative air humidity 35−70%, 10−15 air changes per hour, air movement <0.2 m/s) with food and water available ad libitum in the home cage. Animals were used only once in all in vivo models, except for models of mononeuropathy, for which they were tested repeatedly with a washout period of at least 1 week between tests. Apart from the exceptions mentioned below, animal testing was performed in accordance with the recommendations and policies of the International Association for the Study of Pain (Zimmermann, 1983) and the German Animal Welfare Law. All study protocols were approved by the local government committee for animal research, which is advised by an independent ethics committee. Animals were assigned randomly to treatment groups. Different doses and vehicles were tested in a randomized fashion. Although the operators performing the behavioral tests were not formally "blinded" with respect to the treatment, they were not aware of the study hypothesis or the nature of differences between drugs.

Experiments in the bone cancer pain model were conducted in accordance with the International Association for the Study of Pain guidelines and were approved by the Algos Therapeutics Institutional Animal Care and Use Committee (Algos Therapeutics Inc., Saint Paul, MN). Experiments in the side effect models were conducted in accordance with French Animal Welfare Law and were approved by the Centre de Recherches Biologiques Internal Ethics Committee (Baugy, France). For the bone cancer pain and side effect models, animals were assigned randomly to treatment groups. Different doses and vehicles were tested in a randomized and blinded fashion.

Group sizes for the behavioral studies and pharmacological evaluations were as follows: *n* = 10 for the tail-flick, streptozotocin (STZ)-induced diabetic polyneuropathy, spinal nerve ligation (SNL),

and rotarod models; $n = 8$ for the complete Freund's adjuvant (CFA)-induced arthritis and whole-body plethysmography models; $n = 8–14$ for the bone cancer pain model; $n = 13–15$ for the chronic constriction injury (CCI) model; and $n = 4$ for the pharmacokinetic studies.

In Vitro Studies

Receptor Binding Assay. Human MOP, DOP, KOP, and NOP receptor binding assays were run in microtiter plates (Costar 3632; Corning Life Sciences, Tewksbury, MA) with wheat germ agglutinin-coated scintillation proximity assay beads (GE Healthcare, Chalfont St. Giles, UK). Cell membrane preparations of Chinese hamster ovary K1 cells transfected with the human MOP receptor (Art.-No. RBHOMM, lot-No. 307-065-A) or the human DOP receptor (Art.-No. RBHODM, lot-No. 423-553-B), and human embryonic kidney cell line 293 cells transfected with the human NOP receptor (Art.-No. RBHORLM, lot-No. 1956) or the human KOP receptor (Art.-No. 6110558, lot-No. 295-769-A) were purchased from PerkinElmer Life and Analytical Sciences (Boston, MA). [N-allyl-2,3-^{3}H]naloxone and [tyrosyl-3,5-^{3}H]deltorphin II (both purchased from PerkinElmer Life and Analytical Sciences), [^{3}H]Ci-977, and [leucyl-^{3}H]nociceptin (both purchased from GE Healthcare) were used as ligands for the MOP, DOP, KOP, and NOP receptor binding studies, respectively. The K_D values of the radioligands used for the calculation of K_i values are provided as supplemental information (Supplemental Table 1). The assay buffer used for the MOP, DOP, and KOP receptor binding studies was 50 mM Tris-HCl (pH 7.4) supplemented with 0.052 mg/ml bovine serum albumin (Sigma-Aldrich Co., St. Louis, MO). For the NOP receptor binding studies, the assay buffer used was 50 mM HEPES, 10 mM MgCl$_2$, 1 mM EDTA (pH 7.4). The final assay volume of 250 μl/well included 1 nM [^{3}H]naloxone, 1 nM [^{3}H]deltorphin II, 1 nM [^{3}H]Ci-977, or 0.5 nM [^{3}H]nociceptin as a ligand and cebranopadol in dilution series. Cebranopadol was diluted with 25% dimethylsulfoxide (DMSO) in water to yield a final 0.5% DMSO concentration, which also served as a respective vehicle control. Assays were started by the addition of beads (1 mg beads/well), which had been preloaded for 15 minutes at room temperature with 23.4 μg of human MOP membranes, 12.5 μg of human DOP membrane, 45 μg of human KOP membranes, or 25.4 μg of human NOP membranes per 250 μl of final assay volume. After short mixing, the assays were run for 90 minutes at room temperature. The microtiter plates were then centrifuged for 20 minutes at 500 rpm, and the signal rate was measured by means of a 1450 MicroBeta Trilux (PerkinElmer/Wallac GmbH, Freiburg, Germany). Half-maximal inhibitory concentration (IC$_{50}$) values reflecting 50% displacement of [^{3}H]naloxone-, [^{3}H]deltorphin II-, [^{3}H]Ci-977-, or [^{3}H]nociceptin-specific receptor binding were calculated by nonlinear regression analysis. Individual experiments were run in duplicate and were repeated three times in independent experiments.

Rat MOP, KOP, and NOP receptor binding assays were run using membrane suspensions from rat brain without the cerebellum for MOP receptors; without the pons, medulla oblongata, and cerebellum for NOP receptors; and without the pons, medulla oblongata, cerebellum, and cortex for KOP receptors and the following tritium-labeled radioligands: [^{3}H]DAMGO (purchased from PerkinElmer Life and Analytical Sciences) in the MOP receptor assay, [^{3}H]nociceptin in the NOP receptor assay, and [^{3}H]Ci-977 in the KOP receptor assay. The assay buffer used for the binding studies was 50 mM Tris-HCl (pH 7.4) supplemented with 0.05% sodium azide (Sigma-Aldrich Co.). The final assay volume of 250 μl/well included 2 nM [^{3}H]DAMGO, 1 nM [^{3}H]nociceptin, or 1 nM [^{3}H]Ci-977 as a ligand in the MOP, NOP, or KOP receptor assays, respectively, and cebranopadol in dilution series. Cebranopadol was diluted with 25% DMSO in water to yield a final 0.5% DMSO concentration, which also served as a respective vehicle control. The assays were started by the addition of the membrane suspensions and, after short mixing, the assays were run for 90 minutes at room temperature. All incubations were run in triplicate and terminated by rapid filtration under mild vacuum

(Brandel cell harvester type M-24 R; Brandel Inc., Gaithersburg, MD) and two washes of 5 ml of buffer using FP-100 Whatman GF/B filter mats (Whatman Schleicher and Schuell, Keene, NH). The radioactivity of the samples was counted after a stabilization and extraction period of at least 15 hours by use of the scintillation fluid Ready Protein (Beckman Coulter GmbH, Krefeld, Germany); the complete competition curves for cebranopadol were recorded.

Off-Target Pharmacology Profile. To obtain a selectivity profile for cebranopadol, its interaction with more than 100 different binding sites (including voltage-gated ion channels, neurotransmitter transporters, ionotropic and metabolic receptors, and enzymes) was tested by BioPrint (Cerep SA, Poitiers, France) according to Cerep standard assay protocols (http://www.cerep.fr/cerep/users/pages/catalog/profiles/catalog.asp).

Agonist-Stimulated [^{35}S]Guanosine-5′-[γ-thio]triphosphate Binding. The [^{35}S]guanosine-5′-[γ-thio]triphosphate (GTPγS) assay was carried out as a homogeneous scintillation proximity assay as described previously (Gillen et al., 2000), with the following modifications. The [^{35}S]GTPγS assay was run in microtiter plates (Costar 3632), in which each well contained 1.5 mg of wheat germ agglutinin-coated scintillation proximity assay beads in a final volume of 200 μl. To test the agonistic activity of cebranopadol on human recombinant MOP, DOP, or NOP receptor-expressing cell membranes from Chinese hamster ovary K1 cells, or KOP receptor-expressing cell membranes from human embryonic kidney cell line 293 cells, 10 μg of membrane proteins per assay was incubated with 0.4 nM [^{35}S]GTPγS (GE Healthcare) and different concentrations of agonists in buffer containing 20 mM HEPES (pH 7.4), 100 mM NaCl, 10 mM MgCl$_2$, 1 mM EDTA, 1 mM dithiothreitol, 1.28 mM NaN$_3$, and 10 μM guanosine diphosphate for 45 minutes at 25°C. The bound radioactivity was determined as previously described (Tzschentke et al., 2007).

In Vivo Studies

Behavioral studies in pain models and pharmacokinetic evaluations were conducted in the laboratories of Grünenthal (Grünenthal GmbH) apart from the studies in the bone cancer model and the side effect models, which were conducted at Algos Therapeutics Inc. and Centre de Recherches Biologiques, respectively, under the sponsorship of Grünenthal GmbH.

Tail-Flick Model of Acute Nociceptive Pain. The tail-flick test was carried out in rats using a modification of the method described by D'Amour and Smith (1941). The tail-flick latency in seconds, the time to withdraw the tail from a radiant heat source (bulb 8V/50W), was measured using a semiautomated device (tail-flick analgesiemeter Typ 50/08/1.bc; Labtec, Dr. Hess, Aachen, Germany). The heat source was adjusted to produce a baseline (BL) tail-flick latency of 3–5 seconds; a cut-off time of 12 seconds was used to prevent tissue damage in animals showing no response. The maximum possible antinociceptive effect was defined as the lack of a tail-flick reaction up to the cut-off time of 12 seconds. The maximum possible effect [% maximum possible effect (MPE)] was calculated according to the formula:

$$\% \text{ MPE} = [(T1 − T0)/(T2 − T0)] \times 100$$

where T0 and T1 are latencies before and after intravenous or oral drug administration, respectively, and T2 is the cut-off time.

CFA-Induced Arthritis Model of Chronic Inflammatory Pain. Rats were anesthetized using 3% isoflurane in oxygen, and the left knee was injected according to Butler and coworkers (1992) with 150 μl of CFA, containing 2 mg/ml of inactivated and dried *Mycobacterium tuberculosis*. The right hind limb joint remained untreated. Animals were assessed for changes in weight bearing 5 days after intra-articular injection using a rat incapacitance tester (Somedic Sales AB, Hörby, Sweden). Rats were placed in the angled Plexiglas chamber of the incapacitance tester with their hind paws on separate sensors, and the percentage body weight distribution was

calculated over a 30-second period. The percentage of contralateral weight bearing was calculated, with 100% values resulting from equal weight distribution across both hind limbs. Data are expressed as % MPE according to the formula:

$$\% \text{ MPE} = [(\text{TP}_S - \text{TP}_0)/(0 - \text{TP}_0)] \times 100$$

where TP_0 is reduction of threat power (%) before substance application, TP_S is reduction of threat power (%) after substance application, and

$$\text{TP}(\%) = 100 - \left\{ (\text{WB}_{ipsi} \times 100)/[(\text{WB}_{ipsi} - \text{WB}_{contra})/2] \right\}$$

where WB_{ipsi} is weight bearing of the ipsilateral paw treated with intra-articular CFA-injection; WB_{contra} is weight bearing of the contralateral untreated paw.

Bone Cancer Pain Model. A rat model of bone cancer pain (Medhurst et al., 2002) was used to induce mechanical hypersensitivity. Rats were anesthetized with 2.5–5.0% isoflurane in oxygen. A small incision was made near the proximal end of the tibia and approximately 1000 mammary gland carcinoma cells were injected into the intramedullary space of the tibia in a 3-μl volume using a Hamilton syringe. The hole in the bone was sealed with Lukens bone wax (Surgical Specialties Corp., Reading, PA), and the skin was closed with wound clips. Experiments were conducted 16–18 days after surgery. BL and post-treatment values for mechanical sensitivity were evaluated using an electronic von Frey (EVF) apparatus (IITC Life Science, Woodland Hills, CA). Reduced maximum force to withdrawal on the ipsilateral relative to the contralateral side is interpreted as a measure of increased mechanical sensitivity. Animals were placed on a wire mesh platform and allowed to acclimatize to their surroundings for a minimum of 30 minutes before testing. The mean of three EVF thresholds was determined for each hind paw per time point. Consecutive testing alternated between ipsilateral and contralateral paws within the testing groups. The mean ± S.E.M. across animals was determined for each treatment group. Animals were tested 60 minutes prior to administration of the test compound or vehicle (BL) and 30, 60, and 180 minutes after administration of the test compound or vehicle. Withdrawal thresholds of the injured ipsilateral paws are expressed as

$$\%\text{MPE} = (\text{Test}_{individual} - \text{BL}_{individual}) \times 100/(\text{BL}_{mean}\text{contra} - \text{BL}_{mean}\text{ipsi}).$$

Withdrawal thresholds of the contralateral paws are expressed as

$$\%\text{MPE} = (\text{Test}_{individual} - \text{BL}_{individual}) \times 100/(\text{BL}_{mean}\text{contra} - \text{BL}_{mean}\text{ipsi}) \times (\text{BL}_{mean}\text{contra}/\text{BL}_{mean}\text{ipsi})$$

A cut off was set at 100% MPE; values above 100% were considered as 100%. The effect of each compound and vehicle was calculated at each postadministration time point as intraindividual % MPE.

STZ-Induced Diabetic Polyneuropathy Model. Rats were injected intraperitoneally with 75 mg/kg STZ (Sigma-Aldrich Chemie GmbH) dissolved in citrate solution (0.1 M citric acid and 0.2 M $\text{Na}_2\text{HPO}_4 \times 2\text{H}_2\text{O}$, with final volume to volume of 53.7/46.3 and final pH of 4.6). Diabetes was confirmed 1 week later by measurement of tail vein blood glucose level by Haemo-Glukotest 20R-800R (Boehringer Mannheim GmbH, Mannheim, Germany) and a reflectance colorimeter (Hestia Pharma GmbH, Mannheim, Germany). Rats with a final blood glucose level of at least 17 mM were considered diabetic and were included in the study. Control animals were treated with citrate solution. Rats were submitted to the paw pressure test previously described by Randall and Selitto (1957). Mechanical nociceptive thresholds were assessed using an Algesiometer (Ugo Basile Srl, Comerio, Italy) by measuring withdrawal thresholds to an increasing pressure stimulus onto the dorsal surface of the right hind paw. The maximum pressure was set at 500*g*, and the endpoints were paw withdrawal, vocalization, or

overt struggling. Tests took place during week 3 after the induction of diabetes. The mechanical nociceptive threshold was measured 30 minutes before injection of the test compound or vehicle, and 15, 30, 45, and 60 minutes after administration of the test compound or vehicle in both diabetic and control animals. Antihyperalgesic efficacy was shown as withdrawal thresholds of the diabetic animals, expressed as

$$\%\text{MPE} = (\text{Test}_{individual} - \text{BL}_{individual}) \times 100/(\text{BL}_{mean}\text{Citrate} - \text{BL}_{mean}\text{STZ})$$

Antinociceptive efficacy was shown as withdrawal thresholds of the nondiabetic animals, expressed as

$$\%\text{MPE} = (\text{Test}_{individual} - \text{BL}_{individual}) \times 100/(\text{BL}_{mean}\text{Citrate} - \text{BL}_{mean}\text{STZ}) \times (\text{BL}_{mean}\text{Citrate}/\text{BL}_{mean}\text{STZ})$$

A cut-off was set at 100% MPE; values above 100% were considered as 100%. The effect of each compound and the pooled vehicle groups were calculated for each testing time point as intraindividual % MPE.

SNL Model. Under pentobarbital anesthesia (60 m/kg i.p. Narcoren; Merial GmbH, Hallbergmoos, Germany), the L_5/L_6 spinal nerves were tightly ligated according to the method by Kim and Chung (1992). After surgery, the animals were allowed to recover for 1 week. The threshold for tactile allodynia was measured with an EVF anesthesiometer (Somedic). Animals were tested 30 minutes prior to administration of the test compound or vehicle (BL) and 30, 60, and 180 minutes after administration of the test compound or vehicle. The median withdrawal threshold for each animal at a given time was calculated from five individual stimulations with the EVF filament. Withdrawal thresholds of the ipsilateral paw are expressed as % MPE by comparing the BL threshold of the L_5/L_6-ligated animals (= 0% MPE) and the control threshold of the sham animals (= 100% MPE). A cut off was set at 100% MPE; values above 100% were considered as 100%. The effect of each test compound and vehicle was calculated at each postadministration time point as intraindividual % MPE value. In the antagonism experiments, 1.0, 2.15, and 4.64 mg/kg i.p. J-113397 (Grünenthal GmbH), 0.1, 0.3, and 1 mg/kg i.p. naloxone, or vehicle were administered 5 minutes before 1.7 μg/kg i.v. cebranopadol, 8.9 mg/kg i.v. morphine, or vehicle. The animals were tested 30 minutes before and 30, 60, and 180 minutes after drug administration.

Tolerance Development in the CCI Model. Under pentobarbital anesthesia (60 mg/kg i.p.), unilateral multiple ligations were performed at the right common sciatic nerve according to the method by Bennett and Xie (1988). After surgery, the animals were allowed to recover for 1 week. The animals developed cold allodynia, which was stable for at least 6 weeks. Cold allodynia was tested on a metal plate cooled by a water bath to a constant temperature of 4°C. The animals were placed on the cold plate for 2 minutes, and the number of brisk withdrawal reactions was counted. The animals were observed on the cold plate for periods of 2 minutes at 30 minutes before and 30 minutes after administration of test compound or vehicle, and the number of brisk withdrawal reactions was counted. % MPE of each time point was calculated according to the formula:

$$\%\text{MPE} = [(\text{T0} - \text{T1})/\text{T0}] \times 100$$

where T0 and T1 were numbers of paw withdrawal reactions before and after drug administration, respectively. The intraperitoneal route of administration was chosen to avoid tissue damage of the tail veins due to daily dosing. Antiallodynia was measured after administration of cebranopadol on days 1, 3, 5, 8, 12, 15, 17, 19, 22, 24, 26, and 29 and after administration of morphine on days 1 and 11.

Rotarod Test. To investigate potential effects on motor coordination, an adapted rotarod test was performed (Dunham and Miya, 1957; Cartmell et al., 1991) using a constant speed device (rotarod for rats, LE8500; Panlab SLU, Barcelona, Spain). The time that the animals remained on the rod was measured before and after administration of the test compound. One day prior to the experiment,

the animals were trained at a speed of 5 rpm for a maximum of 5 attempts of 1 minute. On the day of the test, the animals were placed on the rod rotating at a speed of 15 rpm. Any animals that fell consistently within 1 minute over 5 consecutive attempts were not included in the study. To determine baseline values, selected animals were placed on the rod rotating at a speed of 15 rpm 3 times in succession. The duration of the longest attempt was considered for analysis (cut-off time: 2 minutes). This measurement was repeated 5 minutes after administration of cebranopadol or its vehicle or 30 minutes after administration of morphine or its vehicle.

Whole-Body Plethysmography. Respiration was measured by whole-body plethysmography (Chand et al., 1993). The day prior to assessment of respiratory parameters, a polyethylene catheter was inserted into the femoral vein (for intravenous administration) or subcutaneously in the back of the rat in the lumbar area (for subcutaneous administration) under sodium pentobarbital (45 mg/kg i.p.) anesthesia. On the study day, the animals were placed in a whole-body plethysmograph (Emka Technologies SA, Paris, France). The administration catheter was connected to a sealed rotating connection device fitted at the top of the plethysmograph, leaving the animal free to move. At least 15 minutes after the start of measurements and stabilization of the respiration signal, the animals were dosed. Measurements continued for 4 hours after dosing. Respiration was measured for a period of 10 seconds at regular 1-minute intervals using the Dataquest ART acquisition and analysis system version 4.1 (Data Sciences International, St, Paul, MN) at a sampling frequency of 500 Hz. Each respiratory cycle was analyzed using RS/1 software version 6.0.1 (Brooks Automation Inc., Chelmsford, MA) to determine the mean value of the following parameters: respiratory rate (cycles per minute), tidal volume (milliliter), peak inspiratory flow (milliliter per second), peak expiratory flow (milliliter per second), inspiration time (millisecond), and expiration time (millisecond). From these parameters, minute volume (milliliter per minute) was calculated as tidal volume × respiratory rate and airway resistance index (Enhanced Pause; PenH units) was calculated from expiration time and peak inspiratory and expiratory flows according to Chong et al. (1998). Each parameter was analyzed immediately before dosing and 10, 15, 30, 60, 90, 120, 180, and 240 minutes after dosing.

Pharmacokinetic Characterization. The pharmacokinetic properties of cebranopadol in rats were investigated after a single intravenous dose of 160 μg/kg cebranopadol. The intravenous dose was administered as a bolus in a volume of 2 ml/kg with a catheter in the vena femoralis. Blood samples (200 μl/sample) were withdrawn via an implanted arterial catheter (arteria carotis) by an automated blood sampling system (Culex; Bioanalytical Systems Inc., West Lafayette, IN) at the following sampling times: 0 (predose), 5, 15, 30, 60, 180, 360, 720, and 1440 minutes after administration. Blood samples were centrifuged, and plasma was separated. Plasma concentrations of cebranopadol were determined using a validated liquid chromatography-tandem mass spectrometry method. The lower limit of quantification for cebranopadol in this method was 0.05 ng/ml using a sample volume of 50 μl of plasma.

Data Analysis

In Vitro Studies. IC_{50} values were calculated using the Figure P computer software version 6.0c (Biosoft, Cambridge, UK), and dissociation constant for inhibitor binding (K_i) values were obtained using the Cheng-Prusoff equation (Cheng and Prusoff, 1973). Equilibrium dissociation constant values were calculated using the Ligand computer software, version 4 (Biosoft, Cambridge, UK).

Tail-flick, Bone Cancer Pain, SNL, CCI, and STZ Diabetic Hyperalgesia Models. Data were analyzed by means of one- or two-factor analysis of variance (ANOVA), with or without repeated measures, depending on the experimental design. Significance of treatment, time, or treatment by time interaction effects was analyzed by means of Wilks' Lambda. In case of a significant treatment effect, pairwise comparisons were performed by post hoc analysis using the Bonferroni test. Results were considered statistically significant if $P <$ 0.05. ED_{25}, ED_{50}, or ED_{75} values and 95% confidence intervals (CIs) were determined at the time of the peak effect by semilogarithmic regression analysis or according to Litchfield and Wilcoxon (1949) based on % MPE data.

CFA-Induced Arthritis Model. Data were analyzed by means of two-factor repeated-measures ANOVA. Significance of treatment, time, or treatment by time interaction effects was analyzed by means of Wilks' Lambda. In case of a significant treatment effect, pairwise comparisons were performed at the different time points using Fisher's least significant difference test followed by a post hoc Dunnett test. Results were considered statistically significant if $P < 0.05$.

Rotarod Test. Results are expressed as median with 25th and 75th percentiles. Effects induced by cebranopadol or morphine were compared with those of their respective vehicles using the Kruskal-Wallis test followed by a nonparametric Mann-Whitney U test (unilateral comparison). Statistical tests were processed using RS/1 software version 6.0.1. Results were considered statistically significant if $P < 0.05$.

Whole-Body Plethysmography. Results were expressed as mean ± S.E.M. Homogeneity between groups of baseline values for the parameters measured was tested using ANOVA. The effects of cebranopadol, morphine, or their vehicles were expressed as percentage of change from baseline values, with the exception of airway resistance index that was expressed as variation (i.e., in PenH units) from baseline values. Statistical analysis was conducted using repeated-measures ANOVA with Newman-Keuls post hoc test in case of significance using RS/1 software version 6.0.1. Results were considered statistically significant if $P < 0.05$.

Drugs and Chemicals

The following drugs were used: cebranopadol hemi-citrate (Grünenthal GmbH), fentanyl citrate (Synopharm GmbH, Barsbüttel, Germany), J-113397 (Grünenthal GmbH), morphine HCl (Merck AG, Darmstadt, Germany), morphine sulfate (Baxter, Cherry Hill, NJ), sodium pentobarbital (Narcoren), naloxone HCl (Sigma-Aldrich Chemie GmbH, Taufkirchen, Germany), nociceptin (NeoMPS, Strasbourg, France), DAMGO (Bachem AG, Bubendorf, Switzerland), SNC 80 (Enzo Life Sciences GmbH, Lörrach, Germany), and U69,593 (Sigma-Aldrich Chemie GmbH). The following chemicals were used: cremophor EL, DMSO, 5% glucose (Sigma-Aldrich Chemie GmbH), saline (Baxter USA; Baxter, Unterschleißheim, Germany).

For the in vivo studies, cebranopadol hemi-citrate was dissolved in 10% DMSO/5% Cremophor EL/85% glucose solution (5%), except for tail-flick and whole-body plethysmography models [5% DMSO in 95% glucose solution (5%)], and the CFA-induced arthritis model [5% DMSO, 5% Cremophor EL in 90% glucose solution (5%)]. Administration volume was 10 ml/kg (tail-flick, rotarod, and whole-body plethysmography models), 1 ml/kg (bone cancer pain model), or 5 ml/kg (all other in vivo models).

Morphine HCl, morphine sulfate, and fentanyl citrate were dissolved in physiologic saline solution. Administration volume was 10 ml/kg (tail-flick model), 2 ml/kg (rotarod and whole-body plethysmography models), or 1 ml/kg (bone cancer pain model).

Unless otherwise indicated, the route of administration for cebranopadol, fentanyl, and morphine was intravenous. Cebranopadol was tested as the hemi citrate salt in all in vitro and in vivo studies. Morphine was tested as the hydrochloride or sulfate salts and fentanyl as the citrate salt. All doses and ED_{50} values indicated in the following sections refer to the respective free base. For simplicity, the salt forms have been omitted from the text.

Results

In Vitro Data

Cebranopadol binds with high affinity (subnanomolar to nanomolar range) to NOP and opioid receptors. Table 1 shows

TABLE 1
Affinity and functional activity of cebranopadol at rat and human NOP, MOP, KOP, and DOP receptors
Inhibition constants (K_i) were determined in radioligand binding assays. Agonistic potencies (EC_{50}) and efficacies relative to selective and fully efficacious agonists at the respective receptors were tested in [^{35}S]GTPγS binding assays. Values are means $\pm$ S.D.

Target	Rat Receptor Subtypes	Human Receptor Subtypes		
	Radioligand Binding	Radioligand Binding	[^{35}S]GTPγS Binding	
	K_i	K_i	EC_{50}[a]	Relative Efficacy[b]
	nM	nM	nM	%
NOP receptor	1.0 ± 0.5 (n = 5)	0.9 ± 0.2 (n = 7)	13.0 ± 2.0 (n = 5)	88.9 ± 3.9 (n = 5)
MOP receptor	2.4 ± 1.2 (n = 4)	0.7 ± 0.3 (n = 7)	1.2 ± 0.4 (n = 5)	103.5 ± 4.7 (n = 5)
KOP receptor	64.0 ± 11.0 (n = 2)	2.6 ± 1.4 (n = 7)	17.0 ± 5.0 (n = 6)	67.2 ± 5.3 (n = 6)
DOP receptor	N.D.	18.0 ± 20.0 (n = 11)	110.0 ± 28.0 (n = 4)	105.0 ± 8.5 (n = 4)

N.D., not done.
[a]Agonistic potencies [EC_{50} (nM)] of the reference compounds nociceptin (NOP receptor), DAMGO (MOP receptor), U69,593 (KOP receptor), and SNC 80 (DOP receptor), were 2.3 ± 0.9 (n = 5), 90.0 ± 38.0 (n = 5), 22.0 ± 6.0 (n = 6), and 4.7 ± 2.1 (n = 4), respectively.
[b]Efficacy of 100% is defined as maximum [^{35}S]GTPγS binding induced by stimulation with the reference compounds.

the K_i of cebranopadol in human NOP, MOP, KOP, or DOP receptor binding assays. Cebranopadol showed the most pronounced binding affinities at human NOP and MOP receptors with subnanomolar inhibitory constants. In addition, cebranopadol showed an ~3- to 4-fold weaker binding affinity in a human KOP receptor binding assay, and an ~20- to 26-fold lower affinity in a human DOP receptor binding assay. A comparable binding profile was observed for rat NOP, MOP, and KOP receptors, again showing high-affinity binding to both NOP and MOP receptors and a lower affinity to the KOP receptor. Binding data for the rat DOP receptor were not determined.

The agonistic activity of cebranopadol at the human NOP, MOP, KOP, or DOP receptors was tested in [^{35}S]GTPγS binding assays with membranes from cells expressing the respective recombinant human receptors. Its potency (EC_{50}, concentration with half-maximum inducible [^{35}S]GTPγS binding) and efficacy (percentage of maximum inducible [^{35}S]GTPγS binding) were compared with the functional activity of the selective NOP receptor agonist nociceptin/orphanin FQ, the MOP receptor-selective enkephalin DAMGO, the KOP receptor-selective agonist U69,593, and the DOP receptor-selective agonist SNC 80. The latter are examples of fully efficacious agonists at the respective receptors in the [^{35}S]GTPγS binding assay and were used as comparators to set 100% relative efficacy with regard to the [^{35}S]GTPγS binding rate at the respective receptors. Cebranopadol showed full agonistic efficacy at the human

MOP and DOP receptors, almost full efficacy at the human NOP receptor, and partial efficacy at the human KOP receptor (Table 1).

Binding affinities to more than 100 neuronal and safety-relevant receptors, ion channels (including hERG), and enzymes tested in an extensive Cerep off-target profile were at least 100 to 1000 times lower than opioid receptor affinities and are considered biologically irrelevant. The only exception was the serotonin 5A (5-HT$_{5A}$) receptor, for which a K_i of 8.7 nM was determined. However, in a functional [^{35}S]GTPγS binding assay with membranes expressing human 5-HT$_{5A}$ receptor, cebranopadol did not show agonistic or signrifcant antagonistic effects at concentrations up to 10.0 μM.

Behavioral Tests

ED_{50} values (95% CI) from all pain models that are described in this section are summarized in Table 2. Morphine data are shown for comparison.

Tail-Flick Model. In the tail-flick test, cebranopadol induced dose-dependent inhibition of heat nociception with ED_{50} values (95% CI) of 5.6 (4.4−7.0) μg/kg i.v. and 25.1 (20.7−30.4) μg/kg p.o. The maximum attainable antinociceptive response was obtained at 17 μg/kg i.v. or 80 μg/kg p.o. Peak effects were attained within 20 minutes after intravenous (Fig. 2) and 90 minutes after oral administration. The oral availability, estimated by calculating the ratio of intravenous versus oral ED_{50} values, was 22.0% for cebranopadol.

TABLE 2
ED_{50} values and 95% CIs for cebranopadol and morphine in animal models of acute and chronic pain

| Pain Model	Route	ED_{50} Value (95% CI)	
		Cebranopadol	Morphine
		$\mu g/kg$	mg/kg
Tail-flick, rat	i.v.	5.6 (4.4–7.0)	1.1 (Tzschentke et al., 2006)
Tail-flick, rat	p.o.	25.1 (20.7–30.4)	55.7 (Tzschentke et al., 2006)
Tail-flick, rat	s.c.	N.D.	1.6 (1.3–2.1)
CFA-induced arthritic pain, rat	i.v.	5.5 (3.2–21.0)	1.0 (Schiene et al., 2011)
Bone cancer pain, rat	i.v.	3.6 (1.6–7.0)	1.3 (0.8–1.9)
SNL-induced neuropathy, rat	i.v.	0.8 (0.5–1.1)	3.7 (Christoph et al., 2007)
STZ-induced neuropathy, rat	i.v.	0.5 (0.2–0.8)	N.D.

N.D., not done.
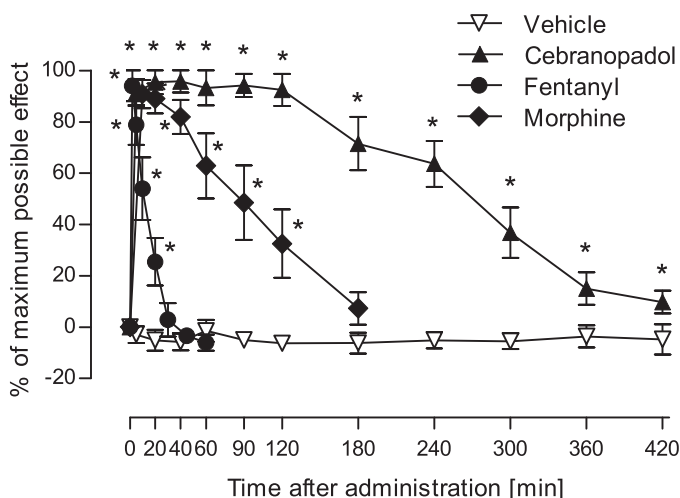
Fig. 2. Duration of action of cebranopadol (12 μg/kg) compared with fentanyl (9.4 μg/kg) and morphine (1.9 mg/kg) after intravenous administration in the rat tail-flick test. Each point of the graph represents the mean $\pm$ S.E.M. of the maximum possible effect; n = 10 animals per group. *$P < 0.05$ versus vehicle. Cebranopadol was tested as hemi-citrate salt, fentanyl was tested as citrate salt, and morphine was tested as hydrochloride salt. Doses refer to the respective free bases.

Equieffective dosages of the high-dose range ($>$80% MPE) were chosen to characterize the duration of action of cebranopadol, fentanyl, and morphine. The duration of action after intravenous administration of 12 μg/kg cebranopadol lasted up to 7 hours, where 10% MPE was measured. The effect of fentanyl and morphine declined within 30 and 180 minutes, respectively (Fig. 2). After oral administration of 55 μg/kg cebranopadol, long-lasting, and significant antinociception was demonstrated for at least 9 hours (last test point measured), where 52% MPE was still attained (data not shown).

CFA-Induced Arthritis Model. Intra-articular CFA injection induced chronic inflammation of the knee joint with a decrease in weight bearing of ~50–60% after 5 days. This t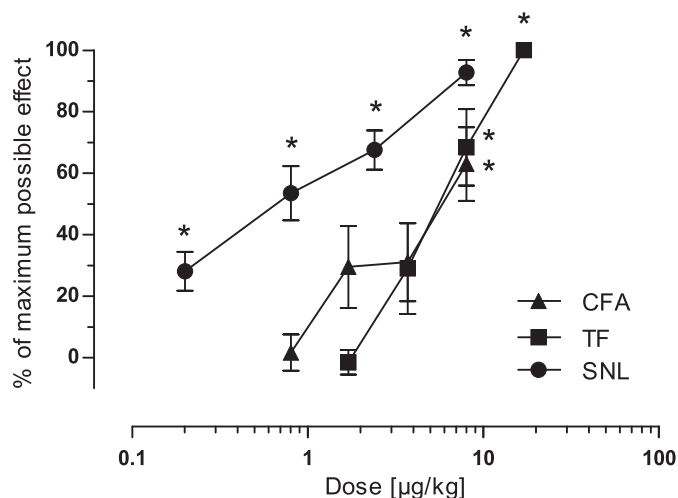ime point coincided with the maximum difference in weight bearing, a state that lasted until 14 days after CFA-injection (data not shown). This reduction in weight bearing was reversed by cebranopadol in a dose-dependent manner, with a maximal effect of 63.0 $\pm$ 11.9% and 65.3 $\pm$ 6.0% after 30 and 60 minutes, respectively, at the dose of 8 μg/kg i.v. (Fig. 3). The calculated ED$_{50}$ (95% CI) was 5.5 (3.2–21.0) μg/kg i.v. 30 minutes after compound administration (Table 2). The ED$_{50}$ was calculated in the dose range from 0.8 to 8.0 μg/kg i.v.

Bone Cancer Pain Model. Intravenous administration of cebranopadol 2.4, 8.0, and 24.0 μg/kg dose-dependently increased ipsilateral paw withdrawal thresholds 30, 60, and 180 minutes after dosing compared with EVF thresholds in vehicle-treated animals. Full efficacy was reached 60 minutes after administration and the resulting ED$_{50}$ value (95% CI) of 3.6 (1.6–7.0) μg/kg i.v. was calculated (Table 2). Contralateral paw withdrawals were increased compared with vehicle-treated animals. However, statistical significance was only reached at the 30- and 60-minute time points for the highest dose tested (Fig. 4).

STZ-Induced Diabetic Polyneuropathy Model. Cebranopadol was tested at 0.24, 0.8, and 2.4 μg/kg i.v. and showed dose-dependent and significant inhibition of mechanical hyperalgesia at all doses tested (Fig. 5). There was no effect on mechanical noxious thresholds in the tested doses because no significant effect was seen in control animals. The calculated ED$_{50}$ (95% CI) was 0.5 (0.2–0.8) μg/kg 30 minutes after administration (Table 2).

SNL Model. Cebranopadol was tested at doses of 0.24, 0.8, 2.4, and 8.0 μg/kg i.v. and showed a dose-dependent inhibition of mechanical hypersensitivity (Fig. 3). The highest dose tested showed full efficacy with 93% MPE. Potency was
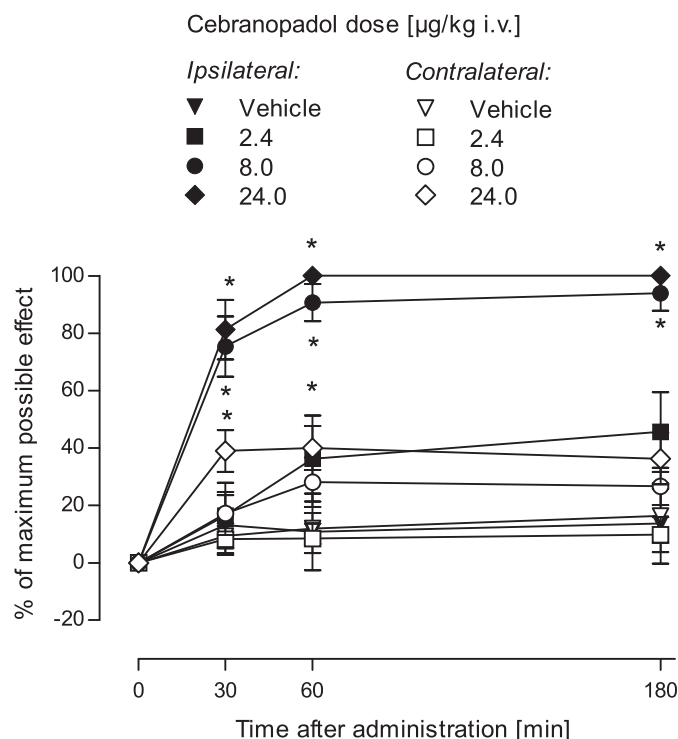

Fig. 3. Analgesic effect of cebranopadol on spinal nerve ligation-induced mononeuropathic pain (SNL) and complete Freund's adjuvant-induced chronic rheumatoid arthritic pain (CFA) 30 minutes after, and on tail flick-induced heat nociception (TF) 20 minutes after intravenous administration. Data are expressed as mean percentage of maximum possible effect $\pm$ S.E.M. (n = 8–10). *$P < 0.05$ versus vehicle.

Fig. 4. Effect of intravenous cebranopadol on mechanical sensitivity in the ipsilateral and contralateral paws in a rat model of bone cancer pain. Data are expressed as percentage of maximum possible effect (mean $\pm$ S.E.M.; n = 10 or 11) on mechanical withdrawal thresholds as measured with an electronic von Frey filament. *$P < 0.05$ versus vehicle.
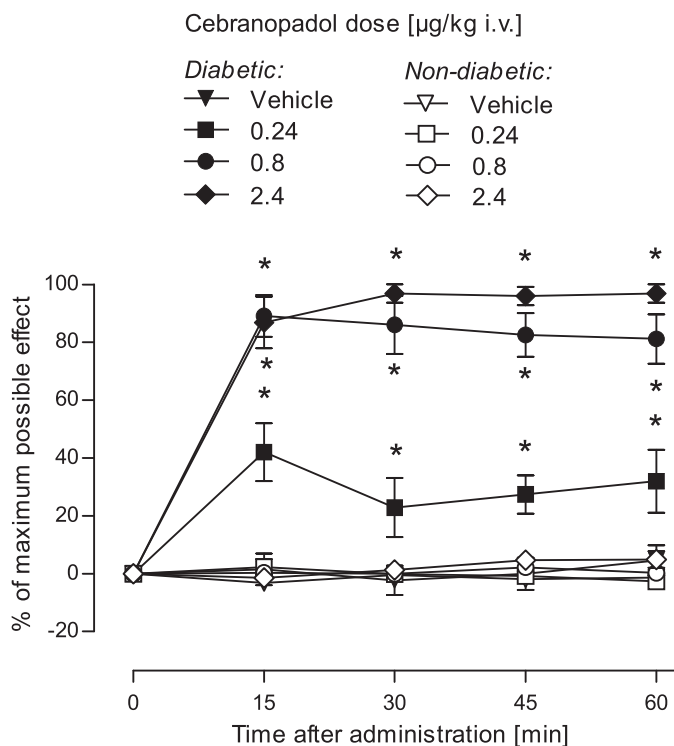
Cebranopadol dose [µg/kg i.v.]

Diabetic: *Non-diabetic:*
▼ Vehicle   ▽ Vehicle
■ 0.24   □ 0.24
● 0.8   ○ 0.8
◆ 2.4   ◇ 2.4

Fig. 5. Antihyperalgesic activity of cebranopadol in streptozotocin (STZ)-treated and control rats measured as % MPE (mean ± S.E.M.; n = 10) by means of a paw pressure test in a model of STZ-induced diabetic polyneuropathy. *P < 0.05 versus vehicle.

quantified by an ED_{50} value (95% CI) of 0.8 (0.5–1.1) µg/kg i.v. calculated from the peak effect versus control values at 30 minutes after administration (Table 2).

Antagonism in the SNL Model. For antagonism studies, cebranopadol 1.7 µg/kg i.v. and morphine 8.9 mg/kg i.v. were tested. These doses were known to be highly efficacious, resulting in >70% MPE. Pretreatment with increasing doses (1.0, 2.15, and 4.64 mg/kg i.p.) of the selective NOP receptor antagonist J-113397 revealed dose-dependent antagonism of the antihypersensitive effect of cebranopadol (Fig. 6A), but no inhibition of the % MPE for morphine (Fig. 6B), suggesting selectivity of the NOP receptor antagonist. Pretreatment with naloxone 1.0 mg/kg i.p., but not with 0.3 mg/kg i.p., resulted in significant antagonism of the antihypersensitive effect of cebranopadol (Fig. 6C). Morphine was dose dependently antagonized by naloxone 0.1–1.0 mg/kg i.p. (Fig. 6D); full antagonism was reached at naloxone 1.0 mg/kg.

Tolerance Development in the CCI Model. Cebranopadol 0.25 and 0.8 µg/kg were chosen as a medium and high dose for the tolerance experiment and were given by intraperitoneal injection once daily (Fig. 7A); allodynia was measured 30 minutes postadministration at multiple time points. Dose-dependent inhibition of cold allodynia was demonstrated. Complete tolerance to cebranopadol had developed by day 22 for the 0.25 µg/kg dose and by day 26 for the 0.8 µg/kg dose. Reference control experiments were performed with morphine dosed daily at 8.9 mg/kg i.p. The number of brisk withdrawal reactions (mean ± S.E.M.) was determined for the
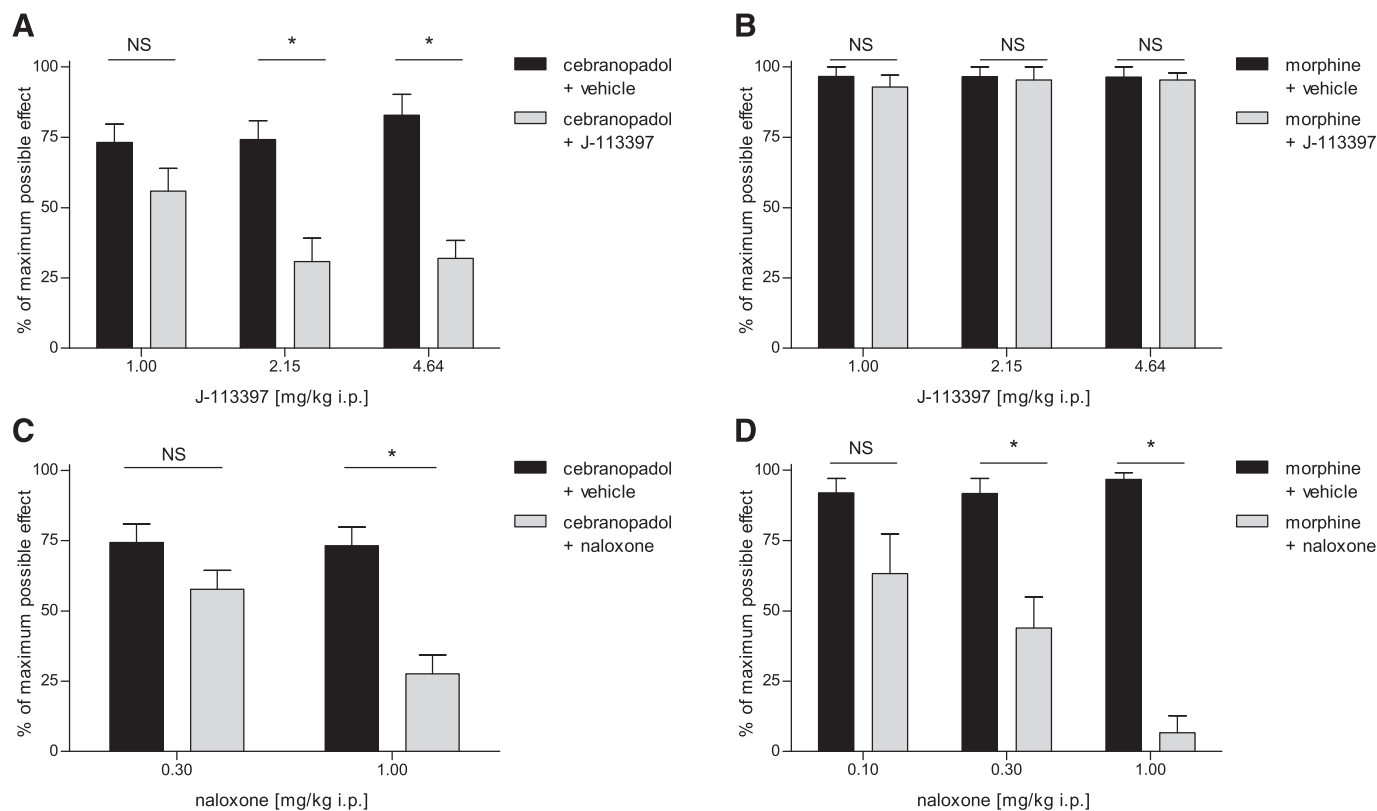

Fig. 6. Effect of 1.0, 2.15, and 4.64 mg/kg i.p. J-113397 on the antihypersensitive effect of 1.7 µg/kg i.v. cebranopadol (A) and 8.9 mg/kg i.v. morphine (B) in the spinal nerve ligation (SNL) model. Effect of 0.3 and 1.0 mg/kg i.p. naloxone on the antihypersensitive effect of 1.7 µg/kg i.v. cebranopadol (C) and of 0.1, 0.3, and 1.0 mg/kg i.p.naloxone on the antihypersensitive effect of 8.9 mg/kg i.v. morphine (D) in the SNL model. Data are given as percentage of maximum possible effect (mean ± S.E.M.; n = 10) measured with an electronic von Frey filament based on the measurement of ipsilateral withdrawal thresholds 30 minutes after administration of cebranopadol or morphine. *P < 0.05 versus vehicle. NS, not significant.
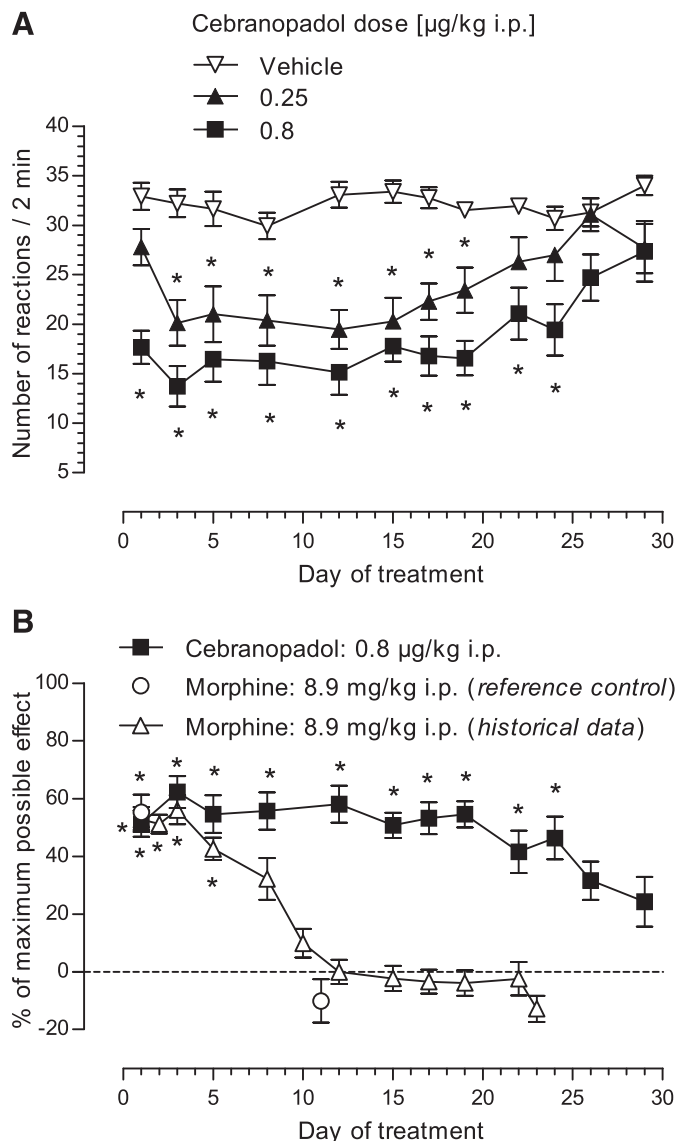
A

B

Fig. 7. Antiallodynic effect of repeated daily intraperitoneal administration of cebranopadol or vehicle as measured by number of paw lifts from a cold plate during 2 minutes (mean ± S.E.M.; n = 13–15) (A) or % MPE (B) in the chronic constriction injury model. *P < 0.05 versus vehicle. Morphine data (8.9 mg/kg i.p.; reference control) with repeated daily administration but measurement of allodynia only on day 1 and day 11 were tested as method control within the same experimental series as cebranopadol. Morphine data (8.9 mg/kg i.p.; historical data) with repeated testing are taken from Tzschentke et al. (2007) and were generated under the same experimental conditions.

vehicle group and the morphine group on day 1 (vehicle 24.0 ± 1.11, morphine 11.0 ± 1.25, P < 0.001) and on day 11 (vehicle 23.0 ± 1.33, morphine 27.0 ± 1.69, P = 0.095), suggesting that full tolerance to morphine had already developed by day 11. Figure 7B shows a comparison in % MPE of the high-dose cebranopadol with morphine and historical morphine data (10 mg/kg i.p.) generated under the same experimental conditions (Tzschentke et al., 2007).

Opioid-Type Side Effects

The side effect profile of cebranopadol was characterized by means of safety pharmacology studies in rats. These studies focused on the CNS and respiratory system as typical target organs for opioid-type side effects.

Rotarod Test. In the rotarod test, cebranopadol was assessed at intravenous doses of 4, 8, and 16 μg/kg. Although these doses produced significant activity in pain models, they did not affect motor coordination (Fig. 8A). In contrast, morphine at intravenous doses of 2.7 and 8.9 mg/kg induced dose-dependent impairment of motor coordination. At these doses, the median time that the animals were able to remain on the rotating rod was significantly decreased from 120 to 52 and 3 seconds, respectively (Fig. 8B).

Whole-Body Plethysmography. A whole-body plethysmography model was used to investigate potential effects of cebranopadol on respiratory function in conscious, freely moving rats. In this model, intravenous administration of vehicle or 4, 8, or 16 μg/kg cebranopadol induced a transient increase in respiratory rate and tidal volume (Fig. 9A). Statistical analysis revealed no significant difference between the treatments during the 4-hour recording period. Consequently, cebranopadol did not significantly alter minute volume at any dose tested (Fig. 9C). Other respiratory parameters, including peak inspiratory and expiratory flows,
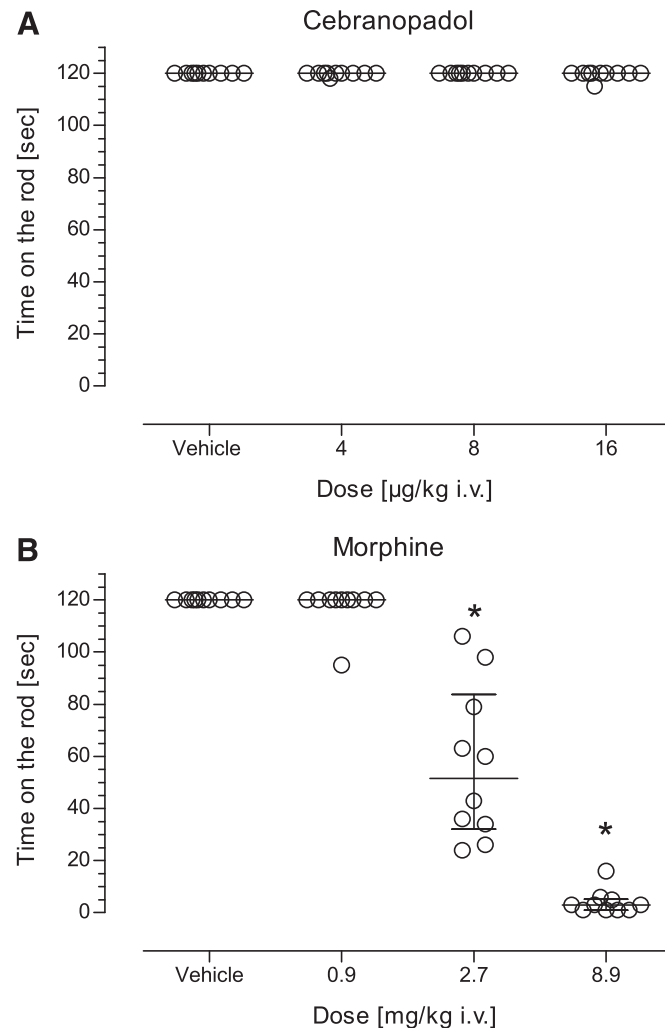
A

B

Fig. 8. Dose-dependent effects of cebranopadol (A) and morphine (B) on motor coordination in rats. Results are expressed as time that the animals remained on the rotarod (individual data, median values with interquartile range; n = 10 animals per group). *P < 0.05 versus vehicle.
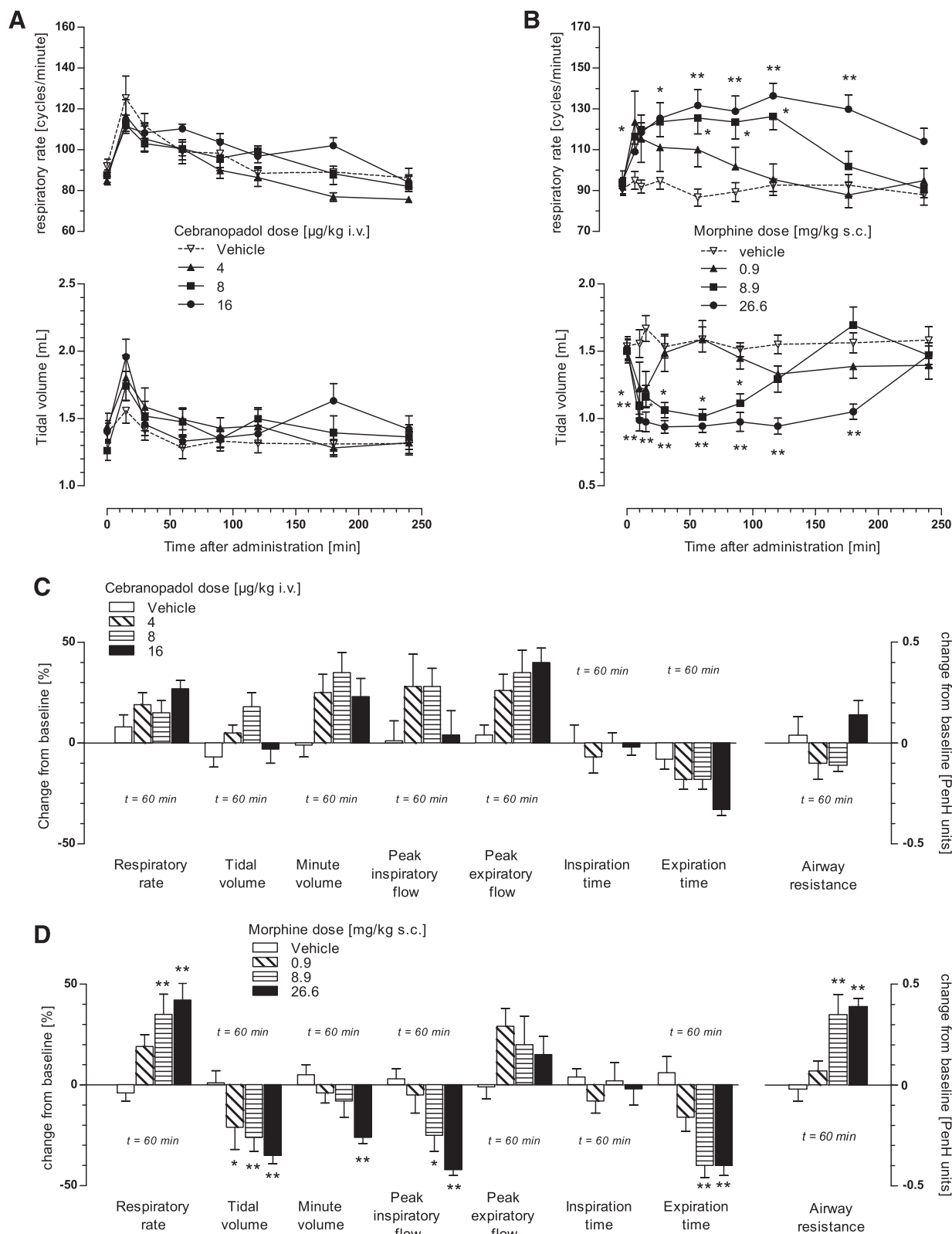
Fig. 9. Effects of cebranopadol (A and C) and morphine (B and D) on respiratory function in the whole-body plethysmography test in conscious rats. (A and B) Time course of effects on respiratory frequency (upper panels) and tidal volume (lower panels) ($n = 8$ animals per group). $*P < 0.05$; $**P < 0.01$ versus vehicle. (C and D) Maximum dose-dependent effects (E_{max}) on respiratory parameters expressed as changes from baseline. Time corresponding to the maximum effect is indicated for each parameter ($n = 8$ animals per group). $*P < 0.05$; $**P < 0.01$ versus vehicle.

inspiration and expiration times, and the calculated airway resistance index were also not significantly changed by administration of cebranopadol (Fig. 9C). The absence of

any effect on respiratory function was in clear contrast to the effects induced by subcutaneous morphine. Increasing doses of morphine 0.9, 8.9, and 26.6 mg/kg s.c. induced a dose-

TABLE 3
Summary (mean ± S.D.) of calculated basic pharmacokinetic parameters of cebranopadol after single intravenous administration to male Sprague-Dawley rats ($n = 4$)

Parameter	160 μg/kg i.v. Cebranopadol
C_0 (ng/ml)	22.8 ± 1.01
AUC (h × ng/ml)	22.2 ± 3.73
$t_{1/2,z}$ (hours)	4.52 ± 0.82
CL (l/kg/h)	7.37 ± 1.38
V_z (l/kg)	47.1 ± 5.34

C_0, extrapolated concentration at the time of intravenous bolus administration ($t = 0$ hours); AUC, area under the plasma concentration-time curve extrapolated to infinity; $t_{1/2,z}$, terminal half-life; CL, total clearance; V_z, apparent volume of distribution during the terminal phase of disposition.

dependent decrease in tidal volume ($E_{max} = -37 ± 8\%$ compared with baseline at 10 minutes after dosing), and a subsequent increase in respiratory frequency by up to $+42 ± 11\%$ at 60 minutes after dosing (Fig. 9B). However, despite the increase in respiratory frequency, minute volume was dose dependently reduced, suggesting a respiratory depressive effect (Fig. 9D). This effect was statistically significant after 26.6 mg/kg s.c. ($E_{max} = -26 ± 3\%$ compared with baseline at 10 minutes after dosing). Respiratory depression induced by morphine also became apparent from dose-dependent increases in intercycle variations in respiratory waveform and increases in the number and duration of pauses in respiratory rhythm (data not shown). In addition, morphine induced statistically significant decreases in peak inspiratory flow ($E_{max} = -42 ± 3\%$ compared with baseline at 10 minutes after dosing) and expiration time ($E_{max} = -40 ± 5\%$ compared with baseline at 60 minutes after dosing), as well as a significant increase in airway resistance index ($E_{max} = +0.39 ± 0.04$ PenH units compared with baseline at 60 minutes after dosing) after 8.9 and 26.6 mg/kg s.c. (Fig. 9D).

Pharmacokinetic Characterization

The pharmacokinetic parameters of cebranopadol after intravenous bolus administration in rats are summarized in Table 3. Cebranopadol was rapidly absorbed and extensively distributed. Oral bioavailability in rats was 13–23%.

Discussion

Cebranopadol, a new chemical entity that is currently in clinical development for the treatment of severe chronic nociceptive and neuropathic pain, was derived from a novel chemical series of spiro[cyclohexane-dihydropyrano[3,4-b]indol]-amines (S. Schunk, K. Linz, C. Hinze, S. Frormann, S. Oberbörsch, B. Sundermann, S. Zemolka, W. Englberger, T. Germann, T. Christoph, B.Y. Kögel, W. Schröder, S. Harlfinger, D. Saunders, A. Kless, H. Schick, and H. Sonnenschein, submitted manuscript). Compounds within this chemical series have been designed and synthetized as combined NOP and opioid receptor agonists. The aim was to develop new drugs that have the analgesic potential of strong opioids but are associated with fewer opioid-type side effects and are thus characterized by a markedly higher therapeutic index.

Cebranopadol binds with nanomolar affinity to the NOP receptor and to the three opioid receptor subtypes. Human receptor binding affinities decrease in the order NOP receptor ~ MOP receptor > KOP receptor > DOP receptor. A comparable relative binding profile was also shown for rat NOP, MOP, and KOP receptors. Cebranopadol has full agonistic activity at human MOP and DOP receptors, near-full activity at the human NOP receptor, and partial activity at the human KOP receptor. Affinities of cebranopadol to neuronal and safety-relevant targets were 100 to 1000 times lower than opioid receptor affinities. The only relatively high affinity determined for cebranopadol was for the 5-HT$_{5A}$ receptor, but this affinity was lower than the affinity to NOP and MOP receptors by approximately 8-fold. In addition, in a functional [^{35}S]GTPγS binding assay, cebranopadol exhibited neither significant agonistic or antagonistic effects at the human 5-HT$_{5A}$ receptor. Therefore, the affinity to this specific receptor is expected to be without biologic relevance.

In rat models of acute, inflammatory, and bone cancer pain, as well as of chronic mono- and polyneuropathic pain, covering mechanical and thermal stimuli, cebranopadol was shown to be highly potent and efficacious. Cebranopadol is characterized by a very long duration of action lasting up to 7 hours after a single intravenous administration, which relates well to its long plasma half-life of approximately 4.5 hours. Effective doses, characterized by ED$_{50}$ values, ranged from approximately 0.5 to 5.6 μg/kg after intravenous administration (see Table 2). Thus, cebranopadol was approximately 180 to 4800 times more potent in these models than the prototypic opioid receptor agonist morphine. Remarkably, the absolute potency of cebranopadol varied between different pain conditions. Potencies were comparable in a tail-flick model of acute nociceptive pain, in a CFA-induced arthritis model of inflammatory pain, and in conditions of hypersensitivity induced by bone cancer. In contrast, potency was approximately 10 times higher in chronic mononeuropathic pain induced by SNL and polyneuropathic pain caused by STZ-induced diabetes. This is in clear contrast to morphine, which has been shown to display similar potency in acute nociceptive, inflammatory, and bone cancer pain models, but to be less potent in chronic neuropathic pain (see Table 2; Schiene et al., 2011; Bian et al., 1999; Christoph et al., 2007; Rashid et al., 2004). The loss of analgesic potency of opioids such as morphine in neuropathic pain states has been attributed to a decreased expression of presynaptic spinal (Kohno et al., 2005; Ossipov et al., 1995) and peripheral MOP receptors (Rashid et al., 2004). The increased analgesic potency of cebranopadol in models of neuropathic pain is in line with data on selective NOP receptor agonists, which have been shown to have a potent and efficacious antihypersensitive effect in rodent neuropathic pain models (Courteix et al., 2004; Obara et al., 2005; Ju et al., 2013; Linz et al., 2013; reviewed in Schröder et al., 2014). Moreover, it was demonstrated that the antinociceptive potency of intrathecally administered nociceptin was greater in mice with diabetic polyneuropathy than in nondiabetic mice (Kamei et al., 1999). An increase in function of the NOP receptor system under these pathophysiological conditions has been attributed to an upregulation of NOP receptors in dorsal root ganglia neurons (Briscini et al., 2002; Chen and Sommer, 2006). This might suggest a clinical benefit of compounds that are agonists at both NOP and opioid receptors over those that are agonists only at opioid receptors. Studies have shown that combining selective NOP and MOP receptor agonists led to coactivation of both receptor systems and to synergism of antiallodynic and antinociceptive effects in rodents (Courteix et al., 2004) and

nonhuman primates (Cremeans et al., 2012), respectively. On the basis of the in vitro binding data, it is expected that agonism at both NOP and MOP receptors may contribute functionally to the analgesic activity of cebranopadol. Antagonism experiments were carried out to elucidate the contribution of NOP and opioid receptor agonism to antihypersensitivity in chronic neuropathic pain. The antihypersensitive activity of cebranopadol in the SNL model could partially be reversed by pretreatment with either the selective NOP receptor antagonist J-113397 (Ozaki et al., 2000) or the opioid receptor antagonist naloxone (Raynor et al., 1994). At the same antagonist doses, J-113397 did not affect the antihypersensitive effect of morphine, whereas naloxone produced full reversal of morphine activity. This observation points to a significant contribution of both NOP receptor and opioid receptor agonism to the antihypersensitive activity of systemic cebranopadol. More detailed analysis will be required to assess a potential intrinsic synergism between both mechanisms of action.

In addition to the synergistic activity of NOP and opioid receptor agonism in analgesia, it was hypothesized that NOP receptor agonism at a supraspinal level may functionally counteract opioid-typical side effects (Ciccocioppo et al., 2000; Lutfy et al., 2001; Shoblock et al., 2005; Rutten et al., 2010). In particular, development of analgesic tolerance, which is a common limitation with chronic opioid treatment (Morgan and Christie, 2011), as well as rewarding effects were shown to be reduced in rodents if a NOP receptor agonist was coadministered with a selective MOP receptor agonist. In the current study, tolerance to the antiallodynic effect of cebranopadol in the CCI model in the rat developed slowly.
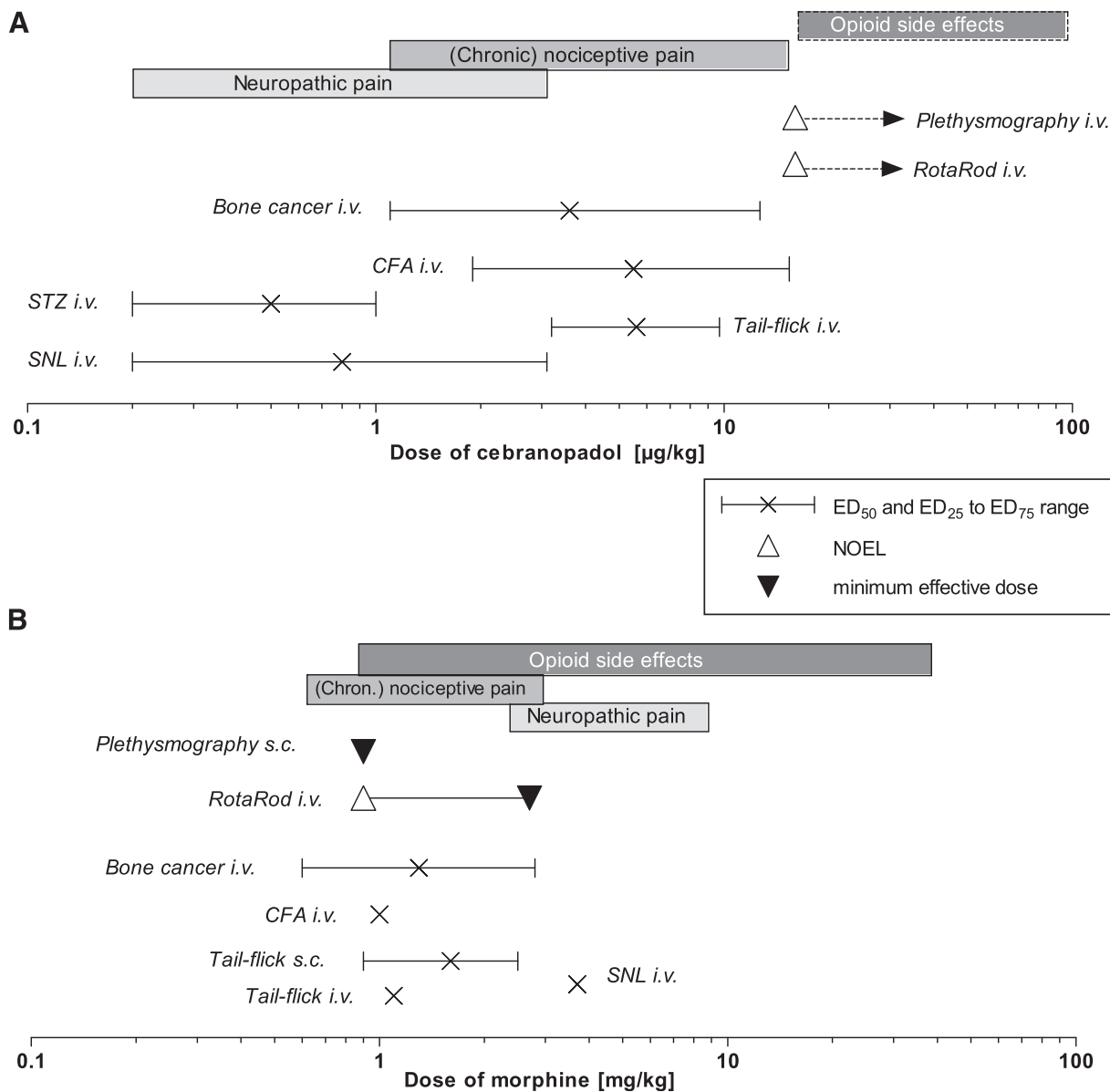

Fig. 10. Comparison of potency and efficacy for cebranopadol (A) and morphine (B) in analgesic and side effect models. ED_{25}, ED_{50}, and ED_{75} values are given for models of analgesia. No observed effect level (NOEL) and/or minimum effective dose values are given for side effect models. Table 2 shows the ED_{50} values for the analgesic models. CFA, Complete Freund's adjuvant-induced chronic rheumatoid arthritic pain; SNL, spinal nerve ligation-induced mononeuropathic pain; STZ, streptozotocin-induced diabetic polyneuropathy.

Complete tolerance against cebranopadol had developed after 22–26 days of repeated daily dosing and was thus significantly delayed compared with morphine, for which complete tolerance occurred under the same experimental conditions after 11 days of repeated daily dosing. The latter data are in accordance with a previous report on the development of tolerance to morphine (Tzschentke et al., 2007). Whether the intrinsic NOP receptor agonism may also reduce or even largely prevent potential reinforcing effects or physical dependence of cebranopadol as postulated for bifunctional NOP and MOP receptor agonists (Toll, 2013) needs further investigation.

To characterize the side effect profile of cebranopadol, safety pharmacology studies were carried out in rats. These focused on typical opioid-type side effects within the CNS and the respiratory system. Opioids such as morphine and oxycodone impair motor coordination within the antinociceptive dose range (Winter et al., 2003), as was confirmed in the present study. In the rotarod test in rats, morphine significantly impaired motor coordination starting at a dose that was approximately two times the ED_{50} for antinociception in the rat tail-flick assay and 0.7 times the ED_{50} for antihypersensitive activity in the rat SNL model (Fig. 10). In contrast, cebranopadol did not induce any effects in the rotarod test, even at the highest test dose of 16 μg/kg i.v., which was at least three times the ED_{50} for antinociception in the tail-flick test and more than 30 times the ED_{50} for antihyperalgesic activity in rats with STZ-induced neuropathic pain (Fig. 10). Comparable observations were made with respect to opioid-type respiratory depression. In a rat whole-body plethysmography model, even at the highest test dose of 16 μg/kg i.v., cebranopadol did not induce significant changes in respiratory parameters. By contrast, in the same model, morphine induced dose-dependent alterations in respiratory parameters that resulted in profound respiratory depression at higher doses. Significant changes in tidal volume had already occurred at doses below the ED_{50} for antinociception in the rat tail-flick assay and the ED_{50} for antihypersensitive activity in neuropathic pain induced by SNL.

In conclusion, cebranopadol displays broad activity in various pain states and is highly potent and efficacious in animal models of acute nociceptive, inflammatory, cancer, and, especially, chronic neuropathic pain. In contrast to opioids such as morphine, cebranopadol displays higher analgesic potency in chronic pain, especially of neuropathic origin, than in acute nociceptive pain. In addition, even after doses higher than those required to induce analgesia, cebranopadol affects neither motor coordination nor respiratory function and thus displays a better tolerability profile than opioids. As a result, there is a broader therapeutic window for cebranopadol than for morphine. As a NOP receptor and opioid receptor agonist, cebranopadol is a novel, first-in-class, potent analgesic under development for the treatment of severe chronic nociceptive and neuropathic pain.

Authorship Contributions

Participated in research design: Linz, Christoph, Schiene, Schröder, De Vry, Jahnel, and Frosch.

Conducted experiments: Linz, Christoph, Schiene, Gautrois, Schröder, Kögel, Beier, and Englberger.

Performed data analysis: Linz, Christoph, Gautrois, and Schröder.

Contributed new reagents or analytic tools: Schunk.

Wrote or contributed to the writing of the manuscript: Linz, Christoph, Tzschentke, Koch, Schiene, Gautrois, and Frosch.

References

Bennett GJ and Xie YK (1988) A peripheral mononeuropathy in rat that produces disorders of pain sensation like those seen in man. *Pain* 33:87–107.

Bian D, Ossipov MH, Ibrahim M, Raffa RB, Tallarida RJ, Malan TP, Jr, Lai J, and Porreca F (1999) Loss of antiallodynic and antinociceptive spinal/supraspinal morphine synergy in nerve-injured rats: restoration by MK-801 or dynorphin antiserum. *Brain Res* 831:55–63.

Briscini L, Corradini L, Ongini E, and Bertorelli R (2002) Up-regulation of ORL-1 receptors in spinal tissue of allodynic rats after sciatic nerve injury. *Eur J Pharmacol* 447:59–65.

Butler SH, Godefroy F, Besson JM, and Weil-Fugazza J (1992) A limited arthritic model for chronic pain studies in the rat. *Pain* 48:73–81.

Calo G and Guerrini R (2013) Medicinal chemistry, pharmacology, and biological actions of peptide ligands selective for the nociceptin/orphanin FQ receptor, in *Research and Development of Opioid-Related Ligands* (Ko MC and Husbands SM, eds) pp 275–325, American Chemical Society, Washington, DC.

Cartmell SM, Gelgor L, and Mitchell D (1991) A revised rotarod procedure for measuring the effect of antinociceptive drugs on motor function in the rat. *J Pharmacol Methods* 26:149–159.

Chand N, Nolan K, Pillar J, Lomask M, Diamantis W, and Sofia RD (1993) Aeroallergen-induced dyspnea in freely moving guinea pigs: quantitative measurement by bias flow ventilated whole body plethysmography. *Allergy* 48:230–235.

Chen Y and Sommer C (2006) Nociceptin and its receptor in rat dorsal root ganglion neurons in neuropathic and inflammatory pain models: implications on pain processing. *J Peripher Nerv Syst* 11:232–240.

Cheng Y and Prusoff WH (1973) Relationship between the inhibition constant (K1) and the concentration of inhibitor which causes 50 per cent inhibition (I50) of an enzymatic reaction. *Biochem Pharmacol* 22:3099–3108.

Chiou LC, Liao YY, Fan PC, Kuo PH, Wang CH, Riemer C, and Prinssen EP (2007) Nociceptin/orphanin FQ peptide receptors: pharmacology and clinical implications. *Curr Drug Targets* 8:117–135.

Chong BT, Agrawal DK, Romero FA, and Townley RG (1998) Measurement of bronchoconstriction using whole-body plethysmograph: comparison of freely moving versus restrained guinea pigs. *J Pharmacol Toxicol Methods* 39:163–168.

Christoph T, Kögel B, Strassburger W, and Schug SA (2007) Tramadol has a better potency ratio relative to morphine in neuropathic than in nociceptive pain models. *Drugs R D* 8:51–57.

Ciccocioppo R, Angeletti S, Sanna PP, Weiss F, and Massi M (2000) Effect of nociceptin/orphanin FQ on the rewarding properties of morphine. *Eur J Pharmacol* 404:153–159.

Courteix C, Coudoré-Civiale MA, Privat AM, Pélissier T, Eschalier A, and Fialip J (2004) Evidence for an exclusive antinociceptive effect of nociceptin/orphanin FQ, an endogenous ligand for the ORL1 receptor, in two animal models of neuropathic pain. *Pain* 110:236–245.

Cox BM, Borsodi A, Caló G, Chavkin C, Christie MJ, Civelli O, Devi LA, Evans C, Henderson G, Höllt V et al.(2009) Opioid receptors: Introduction. Last modified on 13/10/2009. IUPHAR database (IUPHAR-DB). Available from: http://www.iuphar-db.org/DATABASE/FamilyIntroductionForward?familyId=50. Accessed January 24, 2014.

Cremeans CM, Gruley E, Kyle DJ, and Ko MC (2012) Roles of μ-opioid receptors and nociceptin/orphanin FQ peptide receptors in buprenorphine-induced physiological responses in primates. *J Pharmacol Exp Ther* 343:72–81.

D'Amour FE and Smith DL (1941) A method for determining loss of pain sensation. *J Pharmacol Exp Ther* 72:74–79.

Dunham NW and Miya TS (1957) A note on a simple apparatus for detecting neurological deficits in rats and mice. *J Am Pharm Assoc* 46:208–209.

Gillen C, Haurand M, Kobelt DJ, and Wnendt S (2000) Affinity, potency and efficacy of tramadol and its metabolites at the cloned human mu-opioid receptor. *Naunyn Schmiedebergs Arch Pharmacol* 362:116–121.

Jenck F, Wichmann J, Dautzenberg FM, Moreau JL, Ouagazzal AM, Martin JR, Lundstrom K, Cesura AM, Poli SM, and Roever S, et al. (2000) A synthetic agonist at the orphanin FQ/nociceptin receptor ORL1: anxiolytic profile in the rat. *Proc Natl Acad Sci USA* 97:4938–4943.

Ju J, Shin DJ, Na YC, and Yoon MH (2013) Role of spinal opioid receptor on the antiallodynic effect of intrathecal nociceptin in neuropathic rat. *Neurosci Lett* 542:118–122.

Kamei J, Ohsawa M, Kashiwazaki T, and Nagase H (1999) Antinociceptive effects of the ORL1 receptor agonist nociceptin/orphanin FQ in diabetic mice. *Eur J Pharmacol* 370:109–116.

Kim SH and Chung JM (1992) An experimental model for peripheral neuropathy produced by segmental spinal nerve ligation in the rat. *Pain* 50:355–363.

Ko MC, Woods JH, Fantegrossi WE, Galuska CM, Wichmann J, and Prinssen EP (2009) Behavioral effects of a synthetic agonist selective for nociceptin/orphanin FQ peptide receptors in monkeys. *Neuropsychopharmacology* **34**:2088–2096.

Kohno T, Ji RR, Ito N, Allchorne AJ, Befort K, Karchewski LA, and Woolf CJ (2005) Peripheral axonal injury results in reduced mu opioid receptor pre- and post-synaptic action in the spinal cord. *Pain* **117**:77–87.

Labianca R, Sarzi-Puttini P, Zuccaro SM, Cherubino P, Vellucci R, and Fornasari D (2012) Adverse effects associated with non-opioid and opioid treatment in patients with chronic pain. *Clin Drug Investig* **32** (Suppl 1):53–63.

Lambert DG (2008) The nociceptin/orphanin FQ receptor: a target with broad therapeutic potential. *Nat Rev Drug Discov* **7**:694–710.

Linz K, Christoph T, Schiene K, Koch T, and Englberger W (2013). GRT-TA2210, a selective NOP receptor agonist, is active in mouse models of inflammatory and neuropathic pain, in EFIC–8th "Pain in Europe" Congress; 2013 October 9-12; Florence, Italy. Abstract 599. Available from: http://www2.kenes.com/efic2013/scientific/Documents/FinalAbstractbookVersion5.pdf.

Litchfield JT, Jr and Wilcoxon F (1949) A simplified method of evaluating dose-effect experiments. *J Pharmacol Exp Ther* **96**:99–113.

Lutfy K, Hossain SM, Khaliq I, and Maidment NT (2001) Orphanin FQ/nociceptin attenuates the development of morphine tolerance in rats. *Br J Pharmacol* **134**:529–534.

Medhurst SJ, Walker K, Bowes M, Kidd BL, Glatt M, Muller M, Hattenberger M, Vaxelaire J, O'Reilly T, and Wotherspoon G, et al. (2002) A rat model of bone cancer pain. *Pain* **96**:129–140.

Meunier JC, Mollereau C, Toll L, Suaudeau C, Moisand C, Alvinerie P, Butour JL, Guillemot JC, Ferrara P, and Monsarrat B, et al. (1995) Isolation and structure of the endogenous agonist of opioid receptor-like ORL1 receptor. *Nature* **377**:532–535.

Molinari S, Camarda V, Rizzi A, Marzola G, Salvadori S, Marzola E, Molinari P, McDonald J, Ko MC, and Lambert DG, et al. (2013) [Dmt1]N/OFQ(1-13)-NH2: a potent nociceptin/orphanin FQ and opioid receptor universal agonist. *Br J Pharmacol* **168**:151–162.

Monteillet-Agius G, Fein J, Anton B, and Evans CJ (1998) ORL-1 and mu opioid receptor antisera label different fibers in areas involved in pain processing. *J Comp Neurol* **399**:373–383.

Morgan MM and Christie MJ (2011) Analysis of opioid efficacy, tolerance, addiction and dependence from cell culture to human. *Br J Pharmacol* **164**:1322–1334.

Obara I, Przewlocki R, and Przewlocka B (2005) Spinal and local peripheral antiallodynic activity of Ro64-6198 in neuropathic pain in the rat. *Pain* **116**:17–25.

Ossipov MH, Lopez Y, Nichols ML, Bian D, and Porreca F (1995) Inhibition by spinal morphine of the tail-flick response is attenuated in rats with nerve ligation injury. *Neurosci Lett* **199**:83–86.

Ozaki S, Kawamoto H, Itoh Y, Miyaji M, Azuma T, Ichikawa D, Nambu H, Iguchi T, Iwasawa Y, and Ohta H (2000) In vitro and in vivo pharmacological characterization of J-113397, a potent and selective non-peptidyl ORL1 receptor antagonist. *Eur J Pharmacol* **402**:45–53.

Podlesnik CA, Ko MC, Winger G, Wichmann J, Prinssen EP, and Woods JH (2011) The effects of nociceptin/orphanin FQ receptor agonist Ro 64-6198 and diazepam on antinociception and remifentanil self-administration in rhesus monkeys. *Psychopharmacology (Berl)* **213**:53–60.

Randall LO and Selitto JJ (1957) A method for measurement of analgesic activity on inflamed tissue. *Arch Int Pharmacodyn Ther* **111**:409–419.

Rashid MH, Inoue M, Toda K, and Ueda H (2004) Loss of peripheral morphine analgesia contributes to the reduced effectiveness of systemic morphine in neuropathic pain. *J Pharmacol Exp Ther* **309**:380–387.

Raynor K, Kong H, Chen Y, Yasuda K, Yu L, Bell GI, and Reisine T (1994) Pharmacological characterization of the cloned kappa-, delta-, and mu-opioid receptors. *Mol Pharmacol* **45**:330–334.

Reinscheid RK, Nothacker HP, Bourson A, Ardati A, Henningsen RA, Bunzow JR, Grandy DK, Langen H, Monsma FJ, Jr, and Civelli O (1995) Orphanin FQ: a neuropeptide that activates an opioidlike G protein-coupled receptor. *Science* **270**:792–794.

Reiss D, Wichmann J, Tekeshima H, Kieffer BL, and Ouagazzal AM (2008) Effects of nociceptin/orphanin FQ receptor (NOP) agonist, Ro64-6198, on reactivity to acute pain in mice: comparison to morphine. *Eur J Pharmacol* **579**:141–148.

Rosenblum A, Marsch LA, Joseph H, and Portenoy RK (2008) Opioids and the treatment of chronic pain: controversies, current status, and future directions. *Exp Clin Psychopharmacol* **16**:405–416.

Rutten K, De Vry J, Bruckmann W, and Tzschentke TM (2010) Effects of the NOP receptor agonist Ro65-6570 on the acquisition of opiate- and psychostimulant-induced conditioned place preference in rats. *Eur J Pharmacol* **645**:119–126.

Schiene K, De Vry J, and Tzschentke TM (2011) Antinociceptive and antihyperalgesic effects of tapentadol in animal models of inflammatory pain. *J Pharmacol Exp Ther* **339**:537–544.

Schröder W, Lambert D, Ko MC, and Koch T (2014) Functional plasticity of the N/OFQ-NOP receptor system determines analgesic properties of NOP receptor agonists. *Br J Pharmacol* DOI: 10.1111/bph.12744.

Shoblock JR, Wichmann J, and Maidment NT (2005) The effect of a systemically active ORL-1 agonist, Ro 64-6198, on the acquisition, expression, extinction, and reinstatement of morphine conditioned place preference. *Neuropharmacology* **49**:439–446.

Sukhtankar D and Ko MC (2013) Pharmacological investigation of NOP-related ligands as analgesics without abuse liability, in *Research and Development of Opioid-Related Ligands* (Ko MC and Husbands SM, eds) pp 393–416, American Chemical Society, Washington, DC.

Toll L (2013) The use of bifunctional NOP/mu and NOP receptor selective compounds for the treatment of pain, drug abuse, and psychiatric disorders. *Curr Pharm Des* **19**:7451–7460.

Tzschentke TM, Christoph T, Kögel B, Schiene K, Hennies HH, Englberger W, Haurand M, Jahnel U, Cremers TI, and Friderichs E, et al. (2007) (-)-(1R,2R)-3-(3-dimethylamino-1-ethyl-2-methyl-propyl)-phenol hydrochloride (tapentadol HCl): a novel mu-opioid receptor agonist/norepinephrine reuptake inhibitor with broad-spectrum analgesic properties. *J Pharmacol Exp Ther* **323**:265–276.

Tzschentke TM, de Vry J, Terlinden R, Hennies HH, Lange C, Strassburger W, Haurand M, Kolb J, Schneider J, and Buschmann H, et al. (2006) Tapentadol hydrochloride. Analgesic, mu-opioid receptor agonist, noradrenaline reuptake inhibitor. *Drugs Future* **31**:1053–1061.

Winter L, Nadeson R, Tucker AP, and Goodchild CS (2003) Antinociceptive properties of neurosteroids: a comparison of alphadolone and alphaxalone in potentiation of opioid antinociception. *Anesth Analg* **97**:798–805.

Zaveri NT, Jiang F, Olsen C, Polgar WE, and Toll L (2013) Designing bifunctional NOP receptor-mu opioid receptor ligands from NOP receptor-selective scaffolds. Part I. *Bioorg Med Chem Lett* **23**:3308–3313.

Zimmermann M (1983) Ethical guidelines for investigations of experimental pain in conscious animals. *Pain* **16**:109–110.

Zöllner C and Stein C (2007) Opioids. *Handbook Exp Pharmacol* **177**:31–63.

Address correspondence to: Dr. Klaus Linz, Grünenthal GmbH, Preclinical Research and Development, Department of Preclinical Drug Safety, Zieglerstrasse 6, 52078 Aachen, Germany. E-mail: Klaus.Linz@grunenthal.com

Cebranopadol: a Novel Potent Analgesic Nociceptin/Orphanin FQ Peptide and Opioid Receptor Agonist

Klaus Linz, Thomas Christoph, Thomas M. Tzschentke, Thomas Koch, Klaus Schiene, Michael Gautrois, Wolfgang Schröder, Babette Y. Kögel, Horst Beier, Werner Englberger, Stefan Schunk, Jean De Vry, Ulrich Jahnel, and Stefanie Frosch

SUPPLEMENTAL TABLE 1: Inhibition of radioligand binding at rat (*r*) and human (*h*) NOP, MOP, KOP, and DOP receptors by cebranopadol and reference compounds.

Target	Radioligand	K_D [nM]	Unlabeled Ligand	K_i [nM] Mean ± SD	Hill Coefficient (n_H) Mean ± SD
*h*NOP	[^{3}H]Nociceptin	0.22 (n = 2)	Cebranopadol Nociceptin	0.9 ± 0.2 (n = 7) 1.2 ± 1.3 (n = 3)	1.05 ± 0.17 (n = 7) 0.92 ± 0.29 (n = 3)
*h*MOP	[^{3}H]Naloxone	3.43 (n = 2)	Cebranopadol Naloxone	0.7 ± 0.3 (n = 7) 2.5 ± 0.2 (n = 2)	1.58 ± 0.53 (n = 7) 0.96 ± 0.06 (n = 2)
*h*KOP	[^{3}H]Ci-977	0.54 (n = 3)	Cebranopadol U-69,593	2.6 ± 1.4 (n = 7) 5.4 ± 1.8 (n = 3)	0.80 ± 0.19 (n = 7) 0.92 ± 0.10 (n = 3)
*h*DOP	[^{3}H]Deltorphine	2.42 (n = 2)	Cebranopadol SNC 80	18.0 ± 20.0 (n = 11) 1.2 ± 0.1 (n = 3)	1.88 ± 1.40 (n = 11) 0.72 ± 0.07 (n = 3)
*r*NOP	[^{3}H]Nociceptin	0.03 (n = 6)	Cebranopadol Nociceptin	1.0 ± 0.5 (n = 6) 0.5 (n = 1)	1.12 ± 0.17 (n = 6) 0.57 (n = 1)
*r*MOP	[^{3}H]DAMGO	1.2 (n = 4)	Cebranopadol DAMGO	2.4 ± 1.2 (n = 4) 0.1 ± 0.05 (n = 3)	0.90 ± 0.29 (n = 4) 0.86 ± 0.10 (n = 3)
*r*KOP	[^{3}H]Ci977	0.38 (n = 3)	Cebranopadol U-69,593	64.0 ± 11.0 (n = 2) 4.4 ± 2.2 (n = 5)	0.65 ± 0.22 (n = 2) 0.76 ± 0.28 (n = 5)